Miner Deposita (2015) 50:811–824
DOI 10.1007/s00126-014-0571-y

ARTICLE

Characteristics of Cu isotopes from chalcopyrite-rich black smoker chimneys at Brothers volcano, Kermadec arc, and Niuatahi volcano, Lau basin

H. A. Berkenbosch · C. E. J. de Ronde · B. T. Paul · J. B. Gemmell

Received: 19 March 2014 / Accepted: 22 December 2014 / Published online: 1 February 2015

Abstract We analysed primary chalcopyrite from modern seafloor 'black smoker' chimneys to investigate high-temperature hydrothermal Cu isotope fractionation unaffected by metamorphism. Samples came from nine chimneys collected from Brothers volcano, Kermadec arc, and Niuatahi volcano, Lau backarc basin. This is the first known study of Cu isotopes from submarine intraoceanic arc/backarc volcanoes, with both volcanoes discharging significant amounts of magmatic volatiles. Our results (n=22) range from δ^{65}Cu=−0.03 to 1.44±0.18‰ (2 sd), with the majority of samples between ~0.00 and 0.50‰. We interpret this cluster (n=17) of lower δ^{65}Cu values as representing a mantle source for the chimney Cu, in agreement with δ^{65}Cu values for mantle rocks. The few higher δ^{65}Cu values (>0.90‰) occur (1) within the same chimneys as lower values, (2) randomly distributed within the chimneys (i.e. near the top and bottom, interior and exterior), and (3) within chalcopyrite of approximately the same age (<1 year). This suggests the higher δ^{65}Cu values are not related to oxidation by mixing with ambient seawater, but to isotopic variation within the vent fluids over a relatively short time. Theoretical studies demonstrate significant isotopic fractionation can occur between aqueous and vapourous complexing species. When combined with evidence for periodic release of magmatic volatiles at Brothers, we believe vapour transport of Cu is responsible for the observed isotopic fractionation. When compared to global δ^{65}Cu data for primary chalcopyrite, volcanic arc chimneys are most similar to porphyry copper deposits that also form from magmatic-hydrothermal processes in convergent tectonic settings.

Keywords Copper isotopes · Submarine hydrothermal systems · Massive sulphide deposits · Intraoceanic arc · Brothers volcano · Niuatahi volcano

Introduction

Research on copper isotopes has accelerated over the past 15 years, expanding into disciplines as diverse as medicine, archaeology, and geology. Within the latter field, Cu isotopes have been applied to studies of cosmology; environmental science; sedimentology; igneous, metamorphic, and sedimentary rocks; and economic geology. The resulting global database of Cu isotope values may, among other things, elucidate differences between various magma, rock, and/or ore deposit types. This study adds to that body of literature by reporting for the first time Cu isotope measurements from an intraoceanic arc seafloor hydrothermal system, i.e. those from black smoker chimneys hosted by Brothers volcano of the Kermadec arc, as well as from Niuatahi backarc volcano of the Lau basin.

Several hypotheses have been presented on the processes responsible for fractionation of Cu isotopes, such as Cu

Editorial handling: F. Tornos and B. Lehmann

Electronic supplementary material The online version of this article (doi:10.1007/s00126-014-0571-y) contains supplementary material, which is available to authorized users.

H. A. Berkenbosch (✉) · J. B. Gemmell
ARC Centre of Excellence in Ore Deposits (CODES), School of Physical Sciences, University of Tasmania, Private Bag 79, Hobart, Tasmania 7001, Australia
e-mail: heidib1@utas.edu.au

C. E. J. de Ronde
GNS Science, 1 Fairway Drive, Avalon, Lower Hutt 5010, New Zealand

B. T. Paul
School of Earth Sciences, University of Melbourne, Melbourne, Victoria 3010, Australia

complexation, crystallography, and physicochemical parameters such as Eh, pH, and temperature (e.g. Asael et al. 2009; Mathur et al. 2009a; Sherman 2013). The largest fractionations are observed in low-temperature alteration environments. For example, the range of measured Cu isotopes in nature spans from −17 to 10‰, where both ends of this range occur within secondary ore minerals (Mathur et al. 2009a). Not surprisingly, much attention has therefore been paid to economically important supergene mineral deposits and the oxidation of Cu (e.g. Mathur et al. 2005, 2012; Markl et al. 2006; Haest et al. 2009; Braxton and Mathur 2011). Oxidation of Cu(I) in minerals (i.e. chalcopyrite) to aqueous Cu(II) in leachate can cause fractionations of up to 2.7‰ at 40 °C; the leachate may be removed to precipitate ^{65}Cu-enriched deposits, while the residual minerals are ^{65}Cu depleted (Ehrlich et al. 2004; Mathur et al. 2005; Kimball et al. 2009). Rayleigh fractionation and multiple episodes of oxidation and reprecipitation are therefore believed to account for the extreme high and low Cu isotope values in low-temperature environments. Since low-temperature alteration (seafloor weathering) of active sulphide chimneys is relatively minor and does not form supergene deposits, we have largely disregarded secondary alteration processes in this study, consistent with petrographic studies of the chimneys (Berkenbosch et al. 2012a, b). Instead, we focus exclusively on δ^{65}Cu values of primary chalcopyrite and address the possible fractionation mechanisms that may occur during high-temperature processes.

To date, the causes of Cu isotope variation in hypogene depositional environments are poorly understood, with some deposits showing an increase in δ^{65}Cu values with successive intrusions (e.g. Grasberg, Indonesia; Graham et al. 2004), while others have limited variation in δ^{65}Cu values over district-wide scales (e.g. the Schwarzwald district, Germany; Markl et al. 2006). Potential non-redox-driven fractionation processes examined by other workers include equilibrium (or isotope kinetics), variation in source, physicochemical fluid controls, fluid-mineral fractionation during precipitation, and fluid-vapour fractionation (e.g. Graham et al. 2004; Maher and Larson 2007; Li et al. 2010; Maher et al. 2011). Brothers volcano is an ideal site to further examine high-temperature Cu isotope fractionation as it is a hydrothermally active submarine volcano that has been comprehensively studied and where several unaltered, chalcopyrite-rich chimneys have been sampled. Furthermore, seafloor hydrothermal systems related to intraoceanic arc volcanoes are typically shallower and discharge higher concentrations of magmatic volatiles than their mid-ocean ridge (MOR) counterparts (de Ronde et al. 2012), where studies of Cu isotopes related to seafloor mineralization have been focused to date (Zhu et al. 2000; Rouxel et al. 2004). Brothers and Niuatahi chimneys thus provide an alternate, modern tectonic environment to add to, and compare with, the global database of Cu isotope values and are particularly suited to examine the effects of magmatic volatiles on isotopic fractionation.

Geological setting of Brothers volcano

Brothers is one of 30 major submarine volcanoes along the Kermadec arc between New Zealand and Tonga (Fig. 1) and one of only three known to host mineralization (de Ronde et al. 2011). The predominantly dacitic volcano lies to the west of the Kermadec ridge and is situated between major SW-NE-trending faults (Fig. 2a). Embley et al. (2012) detail the morphology and structure of the volcano, regional lineaments, and possible collapse mechanisms for the formation of the large central caldera (3.0×3.4 km). The base of Brothers volcano lies at a water depth of ~2200 m, with the caldera rim situated between depths of ~1420 and 1520 m (de Ronde et al. 2005). The floor of the caldera has a maximum depth of 1879 m. Two volcanic cones occupy the southern half of the caldera: the older, more degraded Lower Cone shoals to 1304 m, whereas the younger Upper Cone shoals to a depth of 1196 m while merging with the southern caldera rim and the southwestern flank of the Lower Cone (Fig. 2a).

Three active vent sites and a fourth extinct one make Brothers the most hydrothermally active volcano along the

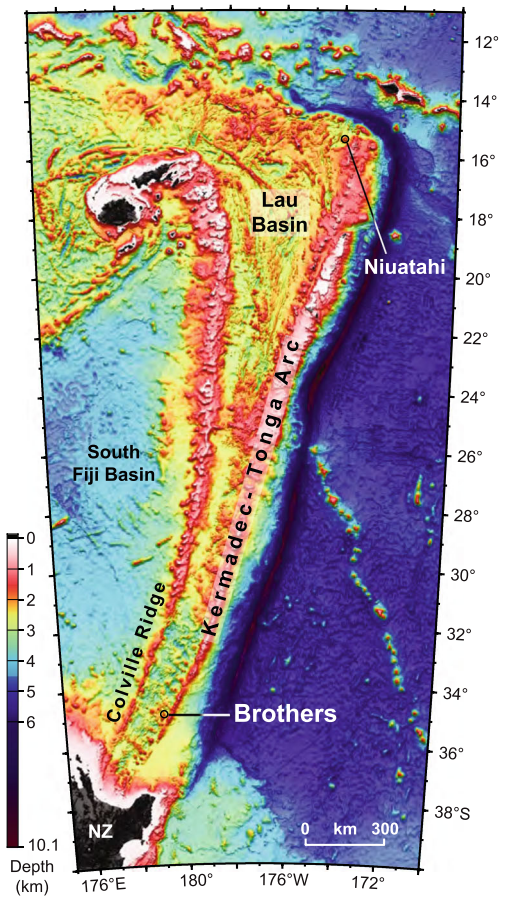

Fig. 1 Map of the ~2500-km-long Kermadec-Tonga arc extending north from New Zealand (*NZ*), showing locations of Brothers and Niuatahi volcanoes. To the east of the arc, at the Kermadec Trench, the Pacific Plate and Louisville seamount chain are subducting westward under the Australian plate

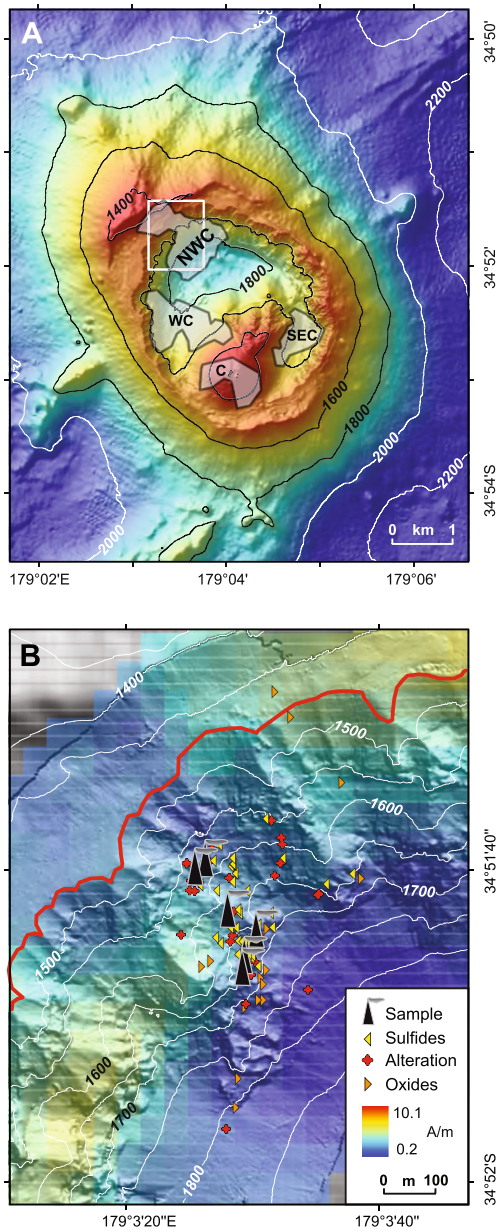

Fig. 2 **a** Bathymetric map of Brothers volcano showing the relationship between intersecting regional SW-NE and SE-NW (the long axis of the volcano) lineaments. The location of the four hydrothermal sites are outlined by their low magnetization anomalies: NW Caldera (*NWC*), West Caldera (*WC*), SE Caldera (*SEC*), and Cone (*C*) (from Caratori Tontini et al. 2012). The *white box* shows the area in **b. b** Bathymetric map of the NW Caldera site overlain by values for magnetization in amperes per meter. The caldera rim is outlined in *red. Dark purple magnetization values* indicate areas of prolonged hydrothermal upflow that destroyed magnetite in the host rock, effectively reducing the magnetization. Submersible observations of hydrothermal manifestations such as sulphide chimneys, oxide crusts, and extensive alteration correspond to the area where the low magnetization anomaly traverses the caldera wall, with sulphides concentrated in the centre of this zone (see *symbols*). Locations of samples used in this study are also shown. Both **a** and **b** are modified after Embley et al. (2012)

Kermadec arc (e.g. Baker et al. 2012). From 1996 to 2005, a series of expeditions utilizing dredges, camera and TV grab tows, miniature autonomous plume recorders (MAPRs), conductivity-temperature-depth-optical (CTDO) tow-yos and casts, and manned submersibles identified and surveyed the gas-rich, diffusely venting Cone site (Fig. 2); the high-temperature, metal-rich NW Caldera site; and the extinct SE Caldera site (e.g. de Ronde et al. 2005, 2011, 2012 and references therein). The similarly high-temperature, metal-rich West Caldera site was only discovered after high-resolution mapping of hydrothermal fluid discharge and magnetic anomalies throughout the caldera by the autonomous underwater vehicles (AUVs) *ABE* in 2007 and *Sentry* in 2011 (Baker et al. 2012; Caratori Tontini et al. 2012). The AUV data further show sparse, high-temperature venting occurring between, and beyond, the boundaries of the main NW and West Caldera sites to cover nearly the entire northern half of the caldera wall, with localized diffuse venting also apparent at the SE Caldera site. Such widespread venting along the caldera walls is primarily controlled by discontinuous ring faults and their intersection with regional lineaments (e.g. de Ronde et al. 2005; Embley et al. 2012). High-resolution magnetic data highlight the longevity of the four hydrothermal sites by delimiting four corresponding zones of low magnetization, the result of prolonged demagnetization of host rocks by the upflow of hot, buoyant, hydrothermal fluids (Fig. 2a; Caratori Tontini et al. 2012).

Due to the drastic differences in venting style, fluid composition, and corresponding mineralization types between the NW Caldera and Cone sites (i.e. largely rock-dominated vs. magmatic-hydrothermal), de Ronde et al. (2011) and Gruen et al. (2012, 2014) modeled the sites as having distinct and contrasting upflow zones. Recorded regional seismicity and local harmonic tremor indicate that the top of the present-day magma chamber lies approximately 2.5 km, and a 'two-phase' zone attributed to the collapse of vapour bubbles ~800 m beneath the Cone site, respectively (Dziak et al. 2008; de Ronde et al. 2011). Magmatic volatiles exsolved from the magma are postulated to rise vertically to be expelled directly on the seafloor at the Cone site, with some mixing with ambient seawater immediately subseafloor. By contrast, pathways beneath the NW Caldera site are considered to be longer and more convoluted leading away from the most recent intrusions beneath the Cone. This ensures greater degrees of water-rock interaction occur as the fluids migrate to the NW Caldera site, where they are incorporated into a hydrothermal circulation cell and then expelled on the seafloor, either as phase-separated brines and/or condensed vapours, to form the metal-rich (Cu-Zn-Au±Pb) chimneys.

Brothers chimneys

This study focuses on samples collected from the NW Caldera vent site (Fig. 2b). High-temperature venting occurs over a

strike length of ~800 m in a SW-NE direction along the caldera walls, between depths of ~1800 and 1550 m; additional diffuse venting occurs on top of the caldera rim at ~1450 m (Baker et al. 2012). Approximately half of the NW Caldera vent field has been surveyed by manned submersibles in 2004 (*Shinkai 6500*) and 2005 (*Pisces V*) and has been described in detail by de Ronde et al. (2005, 2011) and Berkenbosch et al. (2012a). Widespread, white-grey-coloured hydrothermal alteration of lavas and pyroclastics, and Fe-rich amorphous silica crusts and chimneys indicate diffuse venting occurs throughout the field. Over 100 active and inactive chimneys have been surveyed, typically as narrow (<0.5 m diameter), 2–3 m tall spires, but also coalescing into larger, wider structures up to 7 m tall. Individual chimneys may either be relatively straight and smooth-sided or bulbous and sinewy, with many capped by beehive structures. High-temperature venting exiting chimneys in this field typically measured between 265 and 302 °C; other chimneys expelled clear, diffuse fluids of ~35 °C.

Four types of chimneys at the Brothers NW Caldera field were identified by Berkenbosch et al. (2012a). Two are Cu-rich, i.e. chalcopyrite-sulphate and chalcopyrite-bornite chimneys, and two are Zn-rich, i.e. sphalerite-barite and sphalerite-chalcopyrite chimneys. The four types are based on the presence (or absence) of two concentric zones, their thickness, and composition: (1) an inner chalcopyrite layer and (2) an outer sulphate and disseminated sulphide layer. Both Cu-rich chimney types have a thick internal chalcopyrite layer and a sulphate layer of variable thickness composed of anhydrite and barite (Fig. 3). In addition, chalcopyrite-bornite chimneys have an intermediate zone of Cu-enriched phases (i.e. bornite, chalcocite, covellite), which Berkenbosch et al. (2012a) have attributed to seawater weathering (oxidation). However, these authors and de Ronde et al. (2011) also suggested that the suite of bornite, chalcocite, and specular hematite could indicate more oxidized vent fluids, like those characteristic of high sulphidation environments. By contrast, Zn-rich chimneys have a barite-only sulphate layer and either no or trace chalcopyrite.

Niuatahi volcano

We also analysed samples from the Pui ‘O Tafahi chimney collected in 1998 by Nautilus Minerals Inc. from Niuatahi

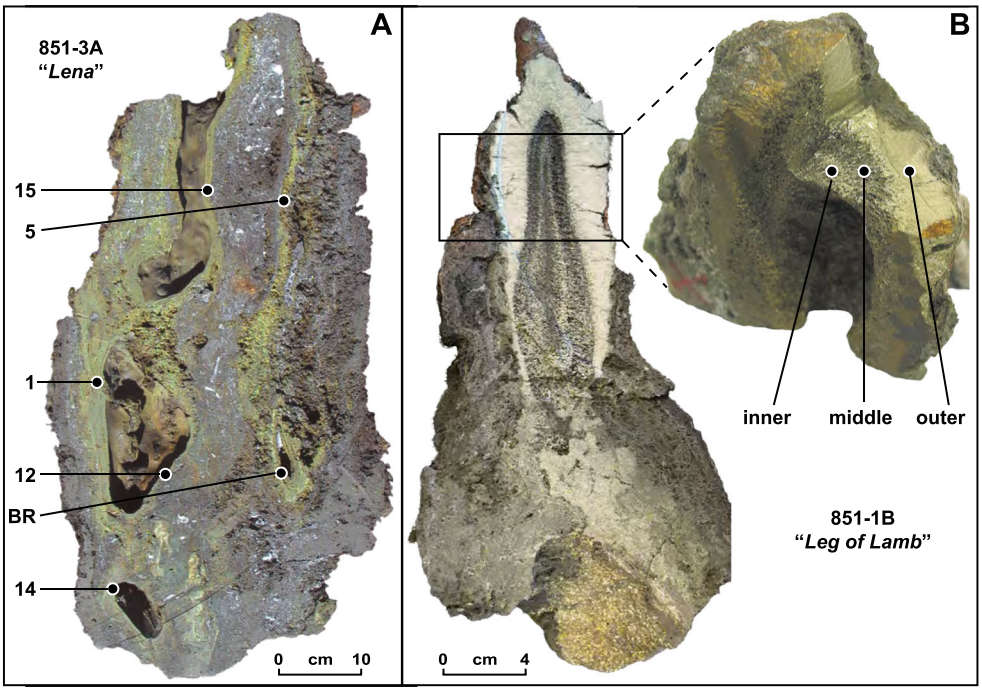

Fig. 3 Two Brothers chimneys used in this study showing locations of individual samples used in the analysis of Cu isotopes. **a** Lena chimney (*851-3A*) is considered to represent the coalescing of two chimneys (de Ronde et al. 2011). On the *left-hand side*, laminated bands of *pale greenish-yellow* chalcopyrite surround a well-defined central orifice, while the poorly defined orifice on the *right-hand side* is comprised of more massive chalcopyrite. Surrounding *grey areas* with white flecks are primarily composed of anhydrite, barite, sphalerite, and pyrite. The lowest and only negative δ^{65}Cu value in this study comes from sample #1 (−0.03‰), while the second highest δ^{65}Cu value comes from sample #14 (1.24‰), only ~25 cm below. *BR* bottom right. **b** Leg of Lamb chimney (*851-1B*) in which the central orifice was in-filled by late ‘box-work’ chalcopyrite in possibly two generations, as given by an internal boundary of thicker chalcopyrite. The *black box* outlines the area from where a smaller sample was sawed off and chalcopyrite analysed in this study (*right-hand side*). Here, the concentric zonation of the orifice is apparent. *Inner* sample indicates a thicker box-work, *middle* sample a thinner box-work, and *outer* sample a massive chalcopyrite. The highest δ^{65}Cu value for this study of 1.44‰ comes from the outer sample, while the two box-work samples had much lower values of 0.18 and 0.13‰, respectively

volcano (previously known as volcano 'O' and MTJ-1; Arculus 2005; Kim et al. 2009, 2011) in the Lau backarc basin (Fig. 1). Niuatahi is a large (~10 km diameter), off-axis caldera volcano located ~90 km west of the Tofua arc or ~45 km E of the NE Lau Spreading Centre. Like Brothers, it is dacitic in composition and has two post-collapse cones located within the caldera, shoaling to ~1300 and ~1500 m depth, respectively. Also similar to Brothers, extensive hydrothermal activity is manifest as high-temperature sulphide deposits along caldera ring faults, with a more magmatic hydrothermal system emplaced on the shallower cone (Kim et al. 2011; Embley et al. 2013). The Pui 'O Tafahi chimney is a very large (~2.5 m length × 1 m diameter) chalcopyrite-sulphate chimney that was recovered from the northern caldera wall. It is primarily comprised of massive chalcopyrite surrounding a chaotic network of internal orifices, with sphalerite- and sulphate-rich zones dominating the exterior.

Methods

In this study, we analysed primary chalcopyrite from Pui 'O Tafahi and the three Brothers chimney types that have Cu-rich mineralization in their cores. Hand samples were crushed and pure chalcopyrite separated by hand picking under a binocular microscope, where possible. A total of 17 samples were processed from eight different Brothers chimneys (Figs. 2b and 3; Table 1), together with five samples from Pui 'O Tafahi.

Copper isotope analysis was undertaken at the Isotope and Trace Element Geochemistry laboratory at the University of Melbourne, under standard clean room conditions. All acids were triple distilled in quartz stills, with all sample containers doubly acid cleaned Teflon Savillex beakers. Approximately 15 mg of each sample was digested in 1 ml inverse aqua regia, dried completely, and then dissolved in 5 ml 7 N HCl in preparation for Cu purification by anion exchange chromatography. The purification method used 2 ml of AG-MP1 resin and followed a procedure modified from Li et al. (2009) by S. Paleri (pers. comm.), as detailed in Table 2. The purified Cu was evaporated to dryness, dissolved in ~2 ml concentrated nitric acid, and then reevaporated. Finally, the residue was dissolved in 2 ml 2 % HNO_3 mass spectrometer run solution and further diluted to an approximately 0.3 μg g^{-1} solution in preparation for isotopic analysis.

Samples were analysed on a Nu-Plasma MC-ICP-MS machine and introduced via an Aridus II desolvating nebulizer. Instrumental mass bias was corrected for by sample—standard bracketing procedures using a solution of NIST SRM 976 copper solution as a reference material. Sample contamination was examined through the analysis of two total procedural blanks (including sample digestion, purification, and mass spectrometry), both of which contributed <0.002 V for ^{63}Cu and ^{65}Cu combined. Reproducibility and accuracy of measurements were estimated through eight analyses of an in-house standard (a homogeneous seafloor hydrothermal sediment) over two sessions that yielded an error of ±0.18‰ (2 sd). Because this uncertainty encompasses the difference in $\delta^{65}Cu$ for all of our duplicate measurements (Table 1), it is the reproducibility we are reporting for this study. Data were reduced using the Iolite software package (Paton et al. 2011) using an in-house data reduction scheme, and results are expressed in standard $\delta^{65}Cu$ notation where

$$\delta^{65}\mathrm{Cu}‰ = \left\{ \frac{\left(^{65}\mathrm{Cu}/^{63}\mathrm{Cu}\right)_{\mathrm{sample}}}{\left(^{65}\mathrm{Cu}/^{63}\mathrm{Cu}\right)_{\mathrm{NIST\ SRM\ 976}}} - 1 \right\} \times 1000.$$

Results

The total range of $\delta^{65}Cu$ values measured in this study is from −0.03 to 1.44±0.18 ‰ (Table 1). The majority (n=17) of the $\delta^{65}Cu$ values cluster within 0.5‰ of each other at the low end of this range (<0.5‰), while a smaller group (n=4) clusters within 0.5‰ of each other at the higher end (>0.9‰; Fig. 4). A single measurement of 0.57‰ lies between these two groups. We measured only relatively high $\delta^{65}Cu$ values for the sphalerite-chalcopyrite chimneys, whereas chalcopyrite-bornite chimneys have both high and low values, and the chalcopyrite-sulphate chimneys have only one high value.

Two individual chimneys have $\delta^{65}Cu$ values in both the groups, i.e. with relatively higher and lower values, but the higher values do not correlate with location inside the chimneys. That is, the highest $\delta^{65}Cu$ value in the Leg of Lamb chimney (851-1B) comes from near the outer margin, at the top, whereas the highest $\delta^{65}Cu$ value from the Lena chimney (#14; 851-3A) comes from the interior conduit, at the base (Fig. 3). The difference in $\delta^{65}Cu$ values over only ~2 cm in the Leg of Lamb chimney is 1.31‰, while the variance is similar (1.25‰) in Lena chimney, though over ~30 cm. Furthermore, that range of $\delta^{65}Cu$ values in Lena chimney occurs within the lining of the internal conduit, and thus in chalcopyrite of approximately the same age (de Ronde et al. 2011). By comparison, the five $\delta^{65}Cu$ values from Pui 'O Tafahi chimney all fall between 0.00 and 0.29‰ despite one sample being located ~80 cm higher in the chimney than the others.

Discussion

The $\delta^{65}Cu$ data for arc-related chimneys is similar to the data from active, basalt-hosted mid-ocean ridge (MOR) chimneys, which range from 0.02 to 1.22 ‰, excepting a single lower value (−0.35‰) from Lucky Strike (Fig. 5). Ultramafic-

Table 1 Sample descriptions and Cu isotope results

Chimney	Depth (mbsl)	Vent fluid temp (°C)	Fragment/ zone	Age (years)	Comments on the chalcopyrite	δ^{65}Cu	Procedural duplicate[a]	Chimney duplicate[b]	Analytical duplicate[c]	Average δ^{65}Cu
Sphalerite-chalcopyrite										
PV-632-11R	1588	–		0.34	Minor tarnishing, slightly spongy, minor sphalerite?	0.561		0.587		0.574
PV-626-4 min	1679	Inactive	a	1.35	Tarnished, spongy, mixed with pyrite and sphalerite.	0.927	0.983			0.955
Chalcopyrite-bornite										
851-1A	1665	302		2.05	Clean, massive.	1.086	0.994 0.935			1.005
851-1B	1665	302	Outer	–	Clean, massive.	1.592	1.386		1.355	1.444
Leg of Lamb			Middle	–	Laths of tarnished chalcopyrite with dirty mineral coating, minor barite?	0.176				0.176
			Inner	1.93	Laths of tarnished chalcopyrite with dirty mineral coating.	0.132				0.132
PV-628-2 min	1577	Inactive		33	Minor tarnishing, minor sphalerite?	0.178				0.178
Chalcopyrite-sulphate										
X573/E	1350–1640	–		–	Rare tarnishing, massive.	0.054		0.064		0.059
852-2B	1627	292	852-2B-a	0.11	Minor tarnishing, slightly spongy.	0.029				0.029
			852-1-a	–	Minor tarnishing, slightly spongy.	0.171	0.224			0.198
			852-1-b	–	Minor tarnishing, massive.	0.032		0.192		0.112
851-3A	1670	274	1	1.39	Rare tarnishing, slightly spongy.	−0.029				−0.029
Lena			5	1.93	Rare tarnishing, slightly spongy.	0.118				0.118
			12	1.01	Rare tarnishing, slightly spongy.	0.355				0.355
			14	–	Rare tarnishing, slightly spongy.	1.244				1.244
			15	–	Moderate tarnishing, spongy, minor anhydrite?	0.354			0.450 0.480	0.428
			BR	–	Rare tarnishing, slightly spongy.	0.329	0.114			0.222
Niuatahi volcano										
Pui 'O Tafahi[d]	?	–	PT-B-7	–	Rare tarnishing, massive.	0.139				0.139
			PT-B-9	–	Finely crushed mixed sulphides, chalcopyrite not separated, no barite.	0.058				0.058
			PT-B-10	–	Finely crushed mixed sulphides, chalcopyrite not separated, no barite.	−0.002				−0.002
			PT-B-11	–	Finely crushed mixed sulphides, chalcopyrite not separated, no barite.	0.286				0.286
			PT-D-9	–	Finely crushed mixed sulphides, chalcopyrite not separated, no barite.	0.250				0.250

Depth, vent fluid temperature, and age data from de Ronde et al. (2011)

– Not measured/analysed, *BR* bottom right

[a] Dissolution, column separation, and isotope analysis performed on a second aliquot of sample powder

[b] Chalcopyrite from the same chimney but of a slightly lower quality

[c] Replicate isotope analysis from the same solution

[d] Samples come from the centre of the chimney either at the base (PT-B) or ~80 cm from the base (PT-D)

Table 2 Protocol for Cu purification by anion exchange

Eluant	Volume (ml)	Purpose
Dilute HCl (~1 N)	~25	Clean column
Concentrated HCl (~12 N)	~25	Clean column
7 N HCl+0.001 % H_2O_2	9.5	Equilibrate column
7 N HCl+0.001 % H_2O_2	0.5	Sample loading
7 N HCl+0.001 % H_2O_2	9	Elution of the bulk sample matrix
7 N HCl+0.001 % H_2O_2	33	Cu peak, left and right shoulder
Dilute HCl (~1 N)	~40	Rinse

Protocol modified from Li et al. (2009) by S. Paleri (pers. comm.)

hosted MOR chimneys also have minimum values near 0‰ but extend to much higher values, i.e. to a maximum of 3.22 ‰. A compilation of δ^{65}Cu values for primary chalcopyrite from other global ore deposits with a known hydrothermal origin shows a dominant peak between −0.50 and 0.75‰, which is entirely consistent with the δ^{65}Cu data presented here (Fig. 6). This cluster of δ^{65}Cu values likely reflects a mantle rock source for Cu in these deposits. For example, published values for whole-rock δ^{65}Cu measurements of basalts are around −0.2‰, while peridotites are between 0.05 and 0.14 ‰ and granites 0.01±0.30‰ (Rouxel et al. 2004; Li et al. 2009; Ikehata and Hirata 2012). Similarly, chalcopyrite from mantle-derived deposits (e.g. Cornwall, England; Bushveld, South Africa; Stillwater, MT, USA) range between −0.15 and 0.21‰ (Zhu et al. 2000; Maher 2005; Maher and Larson

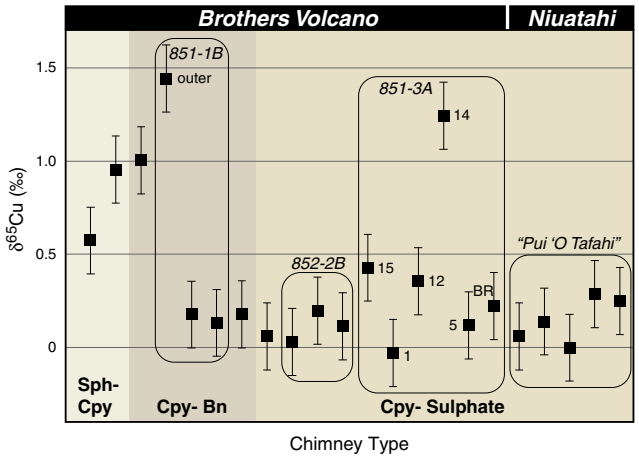

Fig. 4 Scatter plot of δ^{65}Cu value versus chimney type. Multiple samples from the same chimney are enclosed in *boxes*, and labels are given to select data points. The *chimney on the far right* is from Niuatahi. *Error bars* are ±0.18‰ (2 sd). Isotopic values show no discernible trend between chimney types, as the majority of samples fall in the range ~0.0 to 0.5‰, and the few higher values (to ~1.4‰) are found within the same chimney as the relatively lower values. Although sphalerite-chalcopyrite chimneys have no lower values (<0.5‰), two samples are insufficient to determine any correlation. *Sph-Cpy* sphalerite-chalcopyrite, *Cpy-Bn* chalcopyrite-bornite, *Cpy-Sulphate* chalcopyrite-sulphate

2007), while chalcopyrite from two granite-hosted deposits has values of −0.11 and 0.07‰, respectively (Zhu et al. 2000). The consistency of mantle rock δ^{65}Cu values around −0.2 to 0.2‰ suggests that the mantle and associated igneous rocks are relatively homogenous with respect to Cu isotopes. Furthermore, the surface expression of deep source isotopic compositions is not unexpected, as mass-dependent fractionation is minimal when in equilibrium at hydrothermal temperatures ≥300 °C (Larson et al. 2003).

When the data for primary chalcopyrite is divided by ore deposit types, some apparent trends may be insightful with regard to mineralization (Fig. 7). For example, with one exception, active chimneys from arcs, backarcs, and MORs have minimum δ^{65}Cu values of around 0.0‰, likely reflecting the mantle/igneous source. While most hydrothermal ore deposit types have δ^{65}Cu values approaching a normal distribution, active chimneys in both MOR and arc-related environments are skewed towards higher values, suggesting they have been influenced by a Cu isotope enrichment process. The lack of negative δ^{65}Cu values in active chimneys suggests these deposits are separated from the corresponding isotopically depleted part of the system. Inactive chimneys have distinctly depleted δ^{65}Cu values relative to active chimneys and other ore deposit types, implicating seawater oxidation that results in isotopically light (<0‰), residual chalcopyrite and the dispersing of ^{65}Cu-enriched fluids, which could otherwise form a supergene deposit in a subaerial environment. Values of δ^{65}Cu for ancient seafloor volcanic-hosted massive sulphide (VHMS) deposits lie intermediate between modern active and inactive chimneys, displaying a narrow isotopic range, and suggest isotopic homogenization occurs over time for these deposits. Thus, the study of modern seafloor systems may be preferable to ancient massive sulphide deposits with respect to understanding high-temperature Cu isotope fractionation processes.

The distribution of Brothers data is almost exactly the same as that of positive δ^{65}Cu values for porphyry copper deposits (i.e. box and upper whisker; Fig. 7), which have a relatively well-defined, narrow range for a large number of samples (n= 256) and which also form in convergent plate margin settings. In contrast to active black smoker chimneys, the negative δ^{65}Cu values for porphyry copper deposits suggest that they *are* connected to the isotopically depleted part of the system, which extends to the same minimum as inactive chimneys. The near-normal distribution of all ore deposit types implies that ancient deposits in general incorporate both the enriched and depleted parts of the Cu isotope system. Skarn deposits have a similar Cu isotope distribution to porphyry copper deposits, although they extend to a wider range, which is perhaps not surprising considering these deposits utilize similar magmatic-hydrothermal fluids but occur in a greater variety of host rocks.

The consistency between mantle-associated δ^{65}Cu values and the majority of the intraoceanic arc data presented here

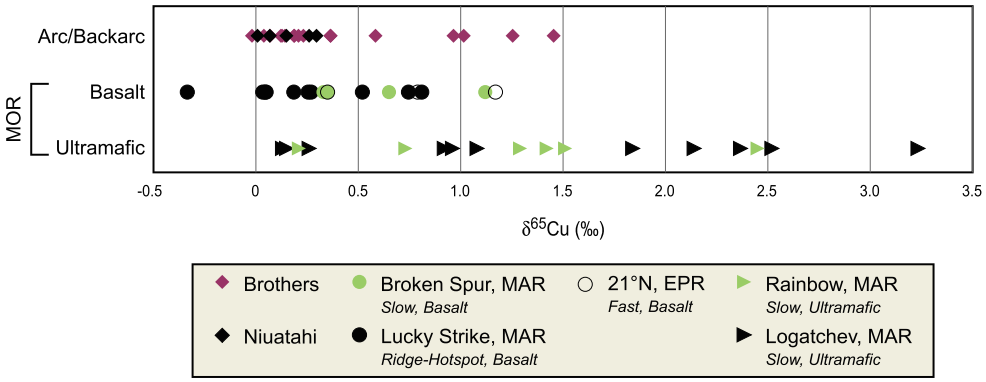

Fig. 5 δ^{65}Cu values for active chimneys from intraoceanic arc and mid-ocean ridge (MOR) environments, distinguished by location. Ridge spreading rate and composition are included in the legend for MOR chimneys. Data largely overlap between the two tectonic environments except for chimneys hosted by ultramafic rocks, which extend to heavier values. *EPR* East Pacific Rise, *MAR* Mid-Atlantic Ridge. MOR data from Zhu et al. (2000) and Rouxel et al. (2004)

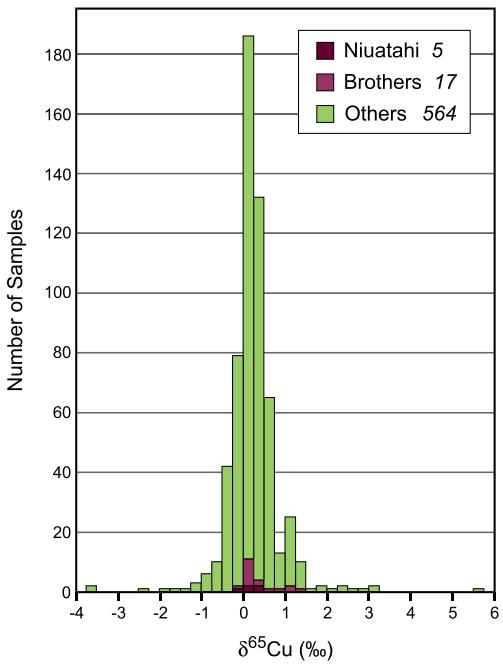

Fig. 6 Histogram of primary chalcopyrite δ^{65}Cu values from Brothers and Niuatahi volcanoes and those from 73 different deposits over 19 countries and the seafloor of two oceans. Regardless of location, primary chalcopyrite typically has δ^{65}Cu values between −0.50 and 0.75‰, with ~88 % of the data points falling within that range. Data from the two arc volcanoes mirrors the general distribution of chalcopyrite δ^{65}Cu values from other worldwide localities, with a consistent peak between 0.00 and 0.25‰, extended to slightly more positive values. The few data points at the ends of the range shown are far from their nearest data point, suggesting that they may not come from primary chalcopyrite, as it can be difficult to distinguish in some deposits. Data from Maréchal et al. (1999), Zhu et al. (2000), Jiang et al. (2002), Larson et al. (2003), Graham et al. (2004), Rouxel et al. (2004), Maher (2005), Mason et al. (2005), Mathur et al. (2005; 2009a; 2009b; 2012; 2013), Markl et al. (2006), Asael et al. (2007), Maher and Larson (2007), Haest et al. (2009), Li et al. (2010), Mirnejad et al. (2010), Braxton and Mathur (2011), Ikehata et al. (2011), and Palacios et al. (2011). See Online Resource 1 for more information on the global data included in this plot, including deposit names and locations

suggests that the few higher δ^{65}Cu values found in the Brothers chimneys result from something other than variation in source values. Similarly, Zhu et al. (2000) considered variations in δ^{65}Cu of ~0.3 to 1.2‰ in active chimneys from a MOR site to originate from a process occurring within the hydrothermal system. That is, the observation that chimneys of the Broken Spur hydrothermal field of the Mid-Atlantic Ridge were isotopically heavier at their base led these workers to propose a process of selective leaching of ^{65}Cu from the host rock, enriching the initial hydrothermal fluids and thus the first precipitated minerals in the chimneys. By contrast, Rouxel et al. (2004) attributed δ^{65}Cu variations of 3.2‰ measured in active MOR chimneys at the Logatchev hydrothermal field, also of the Mid-Atlantic Ridge, to a period of hydrothermal quiescence, whereby subseafloor Cu oxidation and reprecipitation occurred, followed by subsequent renewal of hydrothermal activity. Reduced hydrothermal upflow would facilitate oxidized seawater to penetrate below the seafloor, resulting in an alteration halo of oxidized, ^{65}Cu-enriched phases around a body of ^{65}Cu-depleted chalcopyrite, as seen in the supergene environment. Later resumption of hydrothermal activity then passed new vent fluids around the oxidized exterior margins, partially dissolving them and reprecipitating ^{65}Cu-enriched chalcopyrite at the seafloor. The significance of only those chimneys hosted by ultramafic rocks having δ^{65}Cu values >1.2‰, if any, remains unclear (Rouxel et al. 2004).

The sparse and seemingly random distribution of elevated Cu isotope values within contemporaneous chalcopyrite in Brothers chimneys, however, suggests a more instantaneous fractionation process than those described above. Furthermore, we consider it unlikely that any late hydrothermal upflow would be restricted to contact with the enriched (δ^{65}Cu >0‰) subseafloor halo only and avoid remobilization and reprecipitation of the depleted (δ^{65}Cu <0‰), residual chalcopyrite body as well. Large δ^{65}Cu variations (>1.0‰) are also found within individual chimneys at Rainbow and

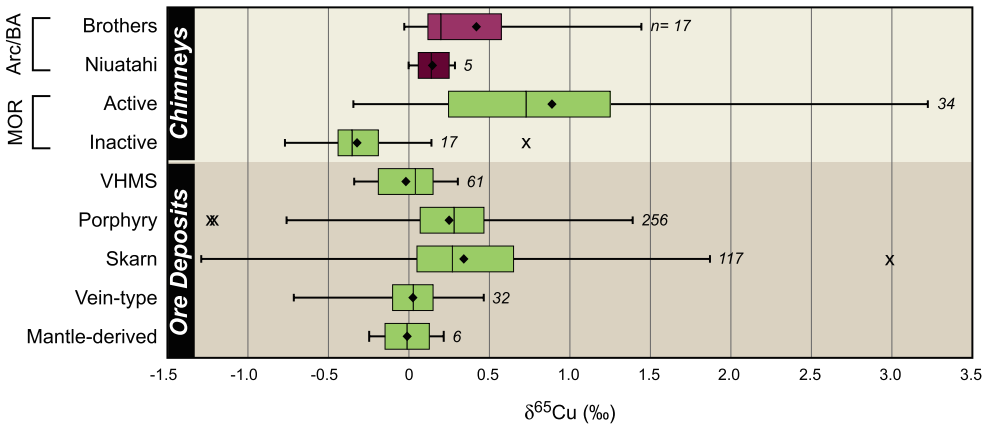

Fig. 7 Statistical box-and-whisker plots that show the distribution of Cu isotopes in primary chalcopyrite for chimneys from this study (*purple*) versus those from active and inactive MOR chimneys, and various hydrothermal ore deposit types (*green*). The *vertical line* inside each box is the median, while the *diamond* (♦) shows the mean. Four outliers (*x*) outside of 3* the interquartile range (length of box) are shown, and a further six outliers are outside the range of this plot for porphyry and vein-type deposits. Some trends within the dominant peak of Fig. 6 become apparent by dividing the data this way, as discussed in the text. Data sources are the same as listed in the caption of Fig. 6. *BA* backarc, *VHMS* volcanic-hosted massive sulphide. The number of data points included in each box-and-whisker is given by the *number on the right-hand side of each plot*

Logatchev hydrothermal fields, suggesting a relatively rapid Cu isotope fractionation process also occurs there. For example, an active chimney at Rainbow had δ^{65}Cu variations of 1.21‰ in the chalcopyrite lining the conduit, while δ^{65}Cu values in another chimney at Logatchev varied by 0.83 and 1.08‰ between the chalcopyrite filling the conduit and that within the chimney wall, respectively (Rouxel et al. 2004). Similarly, Maher and Larson (2007) measured relatively large isotopic variations (δ^{65}Cu=−0.02 to 0.66‰) over ~10 m from a single mineralizing event at the Coroccohuayco skarn deposit, Peru, and suggested fractionation occurred during mineralization.

Copper complexes

We hypothesize that δ^{65}Cu values >0.5‰ in this study reflect isotopic fractionation occurring during transport from deeper sources to the seafloor. Changes in pH, pressure, temperature, salinity, oxygen fugacity, and composition of vent fluids are known to affect the stability of Cu complexes (e.g. Seo et al. 2007; Maher et al. 2011; Rempel et al. 2012; Sherman 2013). Theoretical studies by Seo et al. (2007) and Sherman (2013) calculated the reduced partition function ratios (RPFR) of several Cu ligands to demonstrate that isotopic fractionation occurs between complexing species. Assuming the isotopic character of fluids controls that of minerals (i.e. fractionation is not significant during high-temperature precipitation or equilibrium fluid-mineral fractionation is not achieved), then transportation by different complexes will result in a range of mineral δ^{65}Cu values. The major Cu ligands in high-temperature, low-pH brines are Cl^- and HS^-, with $CuCl_2^-$ and $Cu(HS)_2^-$ the dominant aqueous species (e.g. Seo et al. 2007; Maher et al. 2011; Sherman 2013). Similar RPFR of those dominant complexes would cause minimal fractionation at hydrothermal temperatures of 300 °C (<0.05‰ and either positive or negative depending on the calculation used; Table 3). Even considering increased fractionation at lower temperatures, a maximum difference of only ~0.2‰ exists at the unrealistic temperature of 0 °C. If the minor aqueous Cu complexes $CuCl_3^{2-}$ and $CuHS(H_2O)$ are also considered, the maximum degree of fractionation increases slightly, to ~0.5‰ at 300 °C, equal to the spread of values within the lower group at Brothers. Again, an unrealistic chalcopyrite deposition temperature of ~50 °C must be obtained before fractionations of ~1.4‰ occur between the minor aqueous complexes.

Copper, however, readily enters the vapour phase in sulphuric magmatic-hydrothermal systems (e.g. Lowenstern et al. 1991; Heinrich et al. 1992; Mavrogenes et al. 2002), with vapour complexes modeled by Seo et al. (2007) having higher RPFR than aqueous ones, permitting greater possible degrees of fractionation. The vapourous, hydrated Cu complex $CuCl(H_2O)$, a major species in hydrothermal systems and degassing volcanoes, could cause fractionations of ~0.6‰ from aqueous complexes at 300 °C (Seo et al. 2007; Table 3). Furthermore, vapourous Cu_3Cl_3 has been modeled to fractionate by up to ~1.6‰ compared to aqueous species at 300 °C. Thus, vapour complexes could be *required* to develop the large δ^{65}Cu fractionations measured at Brothers volcano.

Preliminary experimental data, however, contradict the theoretical conclusions of Seo et al. (2007), with two studies suggesting that vapour is ^{65}Cu-depleted compared to fluid. Maher et al. (2011) partially dissolved chalcopyrite with

Table 3 Reduced partition function ratios, 1000*ln(β_{65-63}), for select Cu complexes

Temperature (°C)	Aqueous species					Vapour species	
	$CuCl_3^{2-}$	CuHS	*$CuCl_2^-$*	*$Cu(HS)_2^-$*	$CuHS(H_2O)$	*$CuCl(H_2O)$*	Cu_3Cl_3
0	1.02 (1.26)	1.68	*2.71 (2.79)*	*2.90 (2.72)*	(2.96)	*3.40*	7.85
25	0.85 (1.06)	1.42	*2.29 (2.36)*	*2.46 (2.30)*	(2.50)	*2.89*	6.63
50	0.73 (0.91)	1.22	*1.97 (2.03)*	*2.11 (1.97)*	(2.15)	*2.48*	5.67
100	0.55 (0.68)	0.92	*1.49 (1.53)*	*1.60 (1.49)*	(1.63)	*1.89*	4.29
150	0.43 (0.53)	0.72	*1.17 (1.20)*	*1.25 (1.17)*	(1.28)	*1.48*	3.35
200	0.34 (0.43)	0.58	*0.94 (0.96)*	*1.00 (0.94)*	(1.03)	*1.19*	2.69
300	0.23 (0.29)	0.40	*0.64 (0.66)*	*0.69 (0.64)*	(0.70)	*0.82*	1.84

Dominant complexes are in italics. Data in parenthesis are from Sherman (2013) while those without parenthesis are from Seo et al. (2007)

synthetic hydrothermal solutions and measured Cu isotopes in the residual chalcopyrite, leachate, and reprecipitated Cu considered to have deposited from a vapour phase during quenching. For weakly acidic experiments (i.e. pH 4–6), greater amounts of vapour Cu/fluid Cu generally corresponded to greater negative fractionation (by up to −1.0‰) compared to the original chalcopyrite, indicating a depleted vapour phase relative to the fluid phase. While Maher et al. (2011) acknowledge continued work with better constraints on pH and fO_2 is needed, they concluded that the major control on fractionation is the degree of Cu partitioning between liquid and vapour phases, largely controlled by pH and salinity. Similarly, Rempel et al. (2012) measured the δ^{65}Cu of liquid and vapour pairs in the system CuCl-NaCl-H_2O. Although most pairs had equal δ^{65}Cu values within uncertainties, a shift to heavier isotopic values was noticed between measurements at the highest and lowest pressures, particularly in the experiment with the greatest pressure difference (i.e. with the most vapour removed). Thus, Rayleigh fractionation with periodic removal of ^{65}Cu-depleted vapour was invoked to account for the overall enrichment of the system. However, those experiments were performed at a pH of 9.7 and may vary considerably from realistic hydrothermal conditions of pH<4, considering the effect of pH on vapour complex stability (e.g. Mavrogenes et al. 2002; Maher et al. 2011).

Discrepancy between the experimental and theoretical results may also be due to the hydration of Cu ligands in a hydrothermal system. That is, in steam or a low-density supercritical fluid, the Cu_3Cl_3 complex will most likely be hydrated, although the exact solvation number is not known (Maher et al. 2011; Rempel et al. 2012). Likewise, the hydration number of $CuCl(H_2O)_n$ could range from 2 to 14, depending on the fH_2O at temperatures <400 °C (Migdisov et al. 2014). This will affect the energetics of the molecules and therefore could substantially change the calculated RPFRs. For example, Sherman (2013) recognized that the aqueous CuHS complex in hydrothermal systems is actually in a two-fold coordination as $CuHS(H_2O)$, and the calculated RPFR for that ligand is significantly different from that of unhydrated CuHS (Table 3).

Despite these somewhat inconclusive results, certain field observations are consistent with the theory of ^{65}Cu-enriched vapour transport. For example, Li et al. (2010) used the concept as a viable explanation for spatial δ^{65}Cu patterns of enrichment and depletion noticed in porphyry deposits at Northparkes, Australia. The outward movement and condensation of an enriched vapour could account for peripheral halo δ^{65}Cu values up to ~0.8‰, while depleted brines may form the low δ^{65}Cu margin (minimum≈−0.4‰), when compared to core mineralization (average=0.19±0.14‰). Dilution and dispersion of vapour towards the periphery are also consistent with low Cu grades present there, while concomitant condensation of acidic volatiles at the margin would correlate with an observed shift from K-feldspar to phyllic alteration. Similarly, Maher and Larson (2007) observed that mineralization proximal to fluid sources tended to be isotopically lighter than distal mineralization in the Coroccohuayco and Tintaya skarn deposits of Peru.

Interpretation of magmatic fluids and Cu isotope fractionation

Abundant evidence indicates a substantial magmatic volatile component is included in the hydrothermal systems at Brothers volcano, as detailed by de Ronde et al. (2011). While the Cone site displays the strongest evidence for magmatic contributions, here, we limit our discussion to the NW Caldera site because it is the focus of the Cu mineralization analysed in this study. The most sensitive and unequivocal indicator of magmatic gases is ^{3}He sourced from the mantle (Lupton 1983); highly ^{3}He-enriched plume and vent fluids have been sampled at the NW Caldera site (de Ronde et al. 2005, 2011). Magmatic CO_2 and SO_2 gases would be expected to accompany ^{3}He-enriched discharge at an arc volcano.

Concentrations of CO_2 between 17.3 and 42.8 mM/kg (Massoth et al. 2003; de Ronde et al. 2011) indicate direct injection of magmatic CO_2 when considering concentrations at MOR sites are ≤22 mM/kg (Von Damm 1995). While direct measurements of SO_2 are not possible due to rapid dissolution and disproportionation in water (e.g. Butterfield et al. 2011), high concentrations of the products of those reactions in NW Caldera fluids (end-member H_2S concentrations of 3.8 to $13.6_{(liquid+gas)}$mM/kg and pH values between 2.8 and 3.1) indicate disproportionation of substantial magmatic SO_2 (de Ronde et al. 2011). Isotopic evidence also testifies to a magmatic input; mostly negative δD_{H2O} and $\delta^{15}N$ values, along with measured $\delta^{18}O_{H2O}$ values commonly below 0‰, are all consistent with a magmatic fluid source (Giggenbach 1992; Marty and Dauphas 2003). Enargite-bearing stockwork veins also attest to a high sulphidation environment in the recent past (de Ronde et al. 2005, 2011). Finally, vent fluid Cl concentrations both less than and greater than are indicative of subseafloor phase separation and the subsequent expulsion of condensed gases (de Ronde et al. 2011). Applying hydrological modelling to the NW Caldera site, Gruen et al. (2014) found that the injection of saline magmatic fluids at depth into the hydrothermal system was *required* in order to achieve phase separation. Thus, we consider a process of volatile transport of Cu, with accompanying isotopic fractionation, a distinct possibility to explain the range of $\delta^{65}Cu$ values measured in chimneys sampled from the NW Caldera field.

While Cu isotope analyses were done in this study on a grain-size scale, these techniques cannot detect finer-scale mineralogical and/or chemical fluctuations. For example, trace element mapping of Lena chimney (sample #1) shows visibly laminated chalcopyrite in the interior contains distinct bands, ~30 μm in width, that host a magmatic suite of elements including Co, Mo, Ag, Te, Au, and Bi (Berkenbosch et al. 2012b). Some of these bands are also considered to include magmatic sulphur as de Ronde et al. (2011) noted a correlation between higher Au contents in Brothers chimney chalcopyrite and more negative $\delta^{34}S$ (i.e. more 'magmatic'). If $\delta^{65}Cu$ variations related to vapour influx also occur on such fine scales, it may soon be resolvable using femtosecond LA-ICP-MS with a resolution down to 15 μm (Ikehata et al. 2011). Until then, the Leg of Lamb chimney may better provide insight into the variance of $\delta^{65}Cu$ in different bands, as the banding in this particular chimney is much wider. For example, the outer band (~1.5 cm; Fig. 3b) of massive chalcopyrite has a generally uniform composition characterized by incorporated Se and Au, while the inner bands of later, boxwork chalcopyrite contain no Se or Au (Berkenbosch et al. 2012b). Copper isotopes in the outer band were measured as $\delta^{65}Cu = 1.44$‰, whereas values measured in the inner bands were significantly lower at ~0.15‰. If such large variations in Cu isotopes occur in other, finer bands, such as those seen in Lena chimney, and were randomly sampled during this study, it may explain the large differences in $\delta^{65}Cu$ measured in contemporaneous (<1 year) chalcopyrite that lines the high-temperature, internal conduit of the chimney.

Isotopic analysis of the Leg of Lamb chimney also provides insight into the origin of the bornite-chalcocite-covellite assemblage formed at the exterior margin of the massive chalcopyrite conduit in this chimney. Originally, Berkenbosch et al. (2012a) considered the bornite assemblage to be *secondary* in origin, resulting from weathering of the chalcopyrite core due to its proximity with oxidizing ambient seawater. If this were true, current isotopic studies suggest that the remnant chalcopyrite should have lower values than that of primary chalcopyrite (e.g. Ehrlich et al. 2004; Mathur et al. 2005; Kimball et al. 2009). However, the outer ring of chalcopyrite in the Leg of Lamb chimney has the highest $\delta^{65}Cu$ value measured in this study. Although it is only one sample, this result is not consistent with the bornite assemblage forming from Cu leached from the inner chalcopyrite. Rather, the external Cu phases may well be *primary* and formed due to vent fluids mixing with seawater as proposed, for example, by Haymon (1983) or through the expulsion of more oxidized vent fluids consistent with the injection of magmatic fluids and/or volatiles (de Ronde et al. 2011).

Niuatahi caldera volcano of the Tonga backarc also displays definitive evidence for metal-bearing magmatic vapours, including a pool of metal-rich, molten sulphur atop the largest, central, resurgent volcanic cone (Kim et al. 2011); however, no detailed studies have been undertaken of the northern caldera wall from which the Pui 'O Tafahi chimney was collected. The five samples analysed from that chimney all have relatively low $\delta^{65}Cu$ values, between 0.00 and 0.29‰. The lack of any higher $\delta^{65}Cu$ values may be due to insufficient sampling size or could indicate that magmatic volatiles had less of an influence on the deposition of Cu in this chimney. If the latter, the hydrothermal system along the northern caldera wall may be disconnected from the underlying magmatic source and driven solely by circulating, modified seawater and/or has experienced infrequent injections of magmatic fluids during this chimney's formation.

Conclusions

In summary, we believe the demonstrable magmatic influence on Brothers NW Caldera hydrothermal field is reflected in the Cu isotope values of black smoker chimneys at this site. The bulk of the $\delta^{65}Cu$ data in this study falls between −0.03 and 0.43‰, indicative of mantle rock source values (e.g. Zhu et al. 2000; Li et al. 2009; Ikehata and Hirata 2012). However, a small subset of the data has higher $\delta^{65}Cu$ values, between 0.57 and 1.44‰, which we believe result from relatively rapid

fluctuations of vapour content in the vent fluids. It has been suggested that volcanic degassing could lead to significant Cu partitioning between fluid and vapour phases, with heavy ^{65}Cu modelled to concentrate in the vapour phase and light ^{63}Cu into the liquid phase (Seo et al. 2007). Although the exact Cu ligands involved are uncertain at this time, that ^{65}Cu might concentrate in the vapour phase is consistent with fractionations of ~1.3‰ observed within single chimneys at Brothers volcano, where magmatic contributions are significant, and vapour transport of Cu could be reasonably expected. Repeated, short-lived injections of magmatic volatiles could produce fine-scale bands in chalcopyrite that have varying elemental and isotopic compositions, while relatively longer intervals of vapour injection and/or vapour-favoured pathways may result in the formation of wider bands. Such fluctuating hydrothermal activity is congruous with the ongoing cyclic and dynamic nature of expelled lava, fluid, and gas seen at NW Rota-1 volcano, an erupting and degassing submarine volcano of the Mariana arc (Chadwick et al. 2008). The enriched vapour theory is compatible with models that invoke physicochemical fluctuations to account for Cu isotope fractionation (e.g. Asael et al. 2009), as the stabilities of complexing ligands are sensitive to changes in external conditions. It explains the separation of the isotopically enriched and depleted parts of the system at active seafloor massive sulphide deposits, consistent with the lack of negative $\delta^{65}Cu$ values in active chimneys. It is consistent with the suggestion by several authors that Cu transport by vapour is a common mechanism in the formation of porphyry copper deposits (e.g. Heinrich et al. 1992), which are also known to be distinctly magmatic-hydrothermal in origin and have a similar distribution of positive $\delta^{65}Cu$ values as Brothers (Fig. 7). Moreover, the ^{65}Cu-enrichment of active chimneys from MOR sites suggests vapour transport of Cu may be more prevalent at those environments than previously recognized, although the very high Cu isotope values (>1.5‰) of chimneys hosted in ultramafic rocks may require some additional fractionation process, such as that described by Rouxel et al. (2004). Finally, considering that the distribution of $\delta^{65}Cu$ in primary chalcopyrite from all deposits is concentrated in a relatively narrow band, i.e. between −0.50 and 0.75‰ (Fig. 6), the usefulness of Cu isotopes in fingerprinting distinct mantle reservoirs appears limited.

Acknowledgments This research was supported by an Australian Research Council Centre of Excellence in Ore Deposits (CODES) research scholarship (University of Tasmania), an AusIMM Bicentennial Gold 88 endowment, and a Society of Economic Geologists Foundation student research grant from the Hugh E. McKinstry Fund, all to H. Berkenbosch. C. de Ronde was supported by public research funding from the Government of New Zealand. We thank S.G. Merle for assistance with Figs. 1 and 2 and T. Seward for helpful insight into Cu complexes. This manuscript was also improved by helpful suggestions from R. Mathur and an anonymous reviewer.

References

Arculus RJ (2005) Arc-backarc systems of northern Kermadec-Tonga. Crown Minerals, Ministry of Economic Development, Wellington, pp 45–50, New Zealand Minerals Conference

Asael D, Matthews A, Bar-Matthews M, Halicz L (2007) Copper isotope fractionation in sedimentary copper mineralization (Timna Valley, Israel). Chem Geol 243:238–254. doi:10.1016/j.chemgeo.2007.06.007

Asael D, Matthews A, Oszczepalski S, Bar-Matthews M, Halicz L (2009) Fluid speciation controls of low temperature copper isotope fractionation applied to the Kupferschiefer and Timna ore deposits. Chem Geol 262:147–158. doi:10.1016/j.chemgeo.2009.01.015

Baker ET, Embley RW, de Ronde CEJ, Walker SL (2012) High-resolution hydrothermal mapping of Brothers caldera, Kermadec arc. Econ Geol 107:1583–1593. doi:10.2113/econgeo.107.8.1583

Berkenbosch HA, de Ronde CEJ, Gemmell JB, McNeill AW, Goemann K (2012a) Mineralogy and formation of black smoker chimneys from Brothers submarine volcano, Kermadec arc. Econ Geol 107:1613–1633. doi:10.2113/econgeo.107.8.1613

Berkenbosch HA, de Ronde CEJ, McNeill A, Goemann K, Gemmell JB (2012b) Trace element distribution, with a focus on gold, in copper-rich and zinc-rich sulfide chimneys from Brothers submarine volcano, Kermadec arc. American Geophysical Union Fall Meeting. American Geophysical Union, Washington, DC, San Francisco, pp Abstract OS44A-07

Braxton D, Mathur R (2011) Exploration applications of copper isotopes in the supergene environment: a case study of the Bayugo porphyry copper-gold deposit, southern Philippines. Econ Geol 106:1447–1463. doi:10.2113/econgeo.106.8.1447

Butterfield DA, Nakamura KI, Takano B, Lilley MD, Lupton JE, Resing JA, Roe KK (2011) High SO_2 flux, sulfur accumulation, and gas fractionation at an erupting submarine volcano. Geology 39:803–806. doi:10.1130/g31901.1

Caratori Tontini F, Davy B, de Ronde CEJ, Embley RW, Leybourne MI, Tivey MA (2012) Crustal magnetization of Brothers volcano, New Zealand, measured by autonomous underwater vehicles: geophysical expression of a submarine hydrothermal system. Econ Geol 107:1571–1581. doi:10.2113/econgeo.107.8.1571

Chadwick WW Jr, Cashman KV, Embley RW, Matsumoto H, Dziak RP, de Ronde CEJ, Lau TK, Deardorff ND, Merle SG (2008) Direct video and hydrophone observations of submarine explosive eruptions at NW Rota-1 volcano, Mariana arc. J Geophys Res Solid Earth 113. doi:10.1029/2007jb005215

de Ronde CEJ, Hannington MD, Stoffers P, Wright IC, Ditchburn RG, Reyes AG, Baker ET, Massoth GJ, Lupton JE, Walker SL, Greene RR, Soong CWR, Ishibashi J, Lebon GT, Bray CJ, Resing JA (2005) Evolution of a submarine magmatic-hydrothermal system: Brothers volcano, southern Kermadec arc, New Zealand. Econ Geol 100:1097–1133. doi:10.2113/100.6.1097

de Ronde CEJ, Massoth GJ, Butterfield DA, Christenson BW, Ishibashi J, Ditchburn RG, Hannington MD, Brathwaite RL, Lupton JE, Kamenetsky VS, Graham IJ, Zellmer GF, Dziak RP, Embley RW, Dekov VM, Munnik F, Lahr J, Evans LJ, Takai K (2011) Submarine hydrothermal activity and gold-rich mineralization at Brothers volcano, Kermadec arc, New Zealand. Miner Deposita 46:541–584. doi:10.1007/s00126-011-0345-8

de Ronde CEJ, Butterfield DA, Leybourne MI (2012) Metallogenesis and mineralization of intraoceanic arcs I: Kermadec arc—introduction. Econ Geol 107:1521–1525. doi:10.2113/econgeo.107.8.1521

Dziak RP, Haxel JH, Matsumoto H, Lau TK, Merle SG, de Ronde CEJ, Embley RW, Mellinger DK (2008) Observations of regional seismicity and local harmonic tremor at Brothers volcano, south Kermadec arc, using an ocean bottom hydrophone array. J Geophys Res Solid Earth 113:13. doi:10.1029/2007JB005533

Ehrlich S, Butler I, Halicz L, Rickard D, Oldroyd A, Matthews A (2004) Experimental study of the copper isotope fractionation between aqueous Cu(II) and covellite, CuS. Chem Geol 209:259–269. doi:10.1016/j.chemgeo.2004.06.010

Embley RW, de Ronde CEJ, Merle SG, Davy B, Caratori Tontini F (2012) Detailed morphology and structure of an active submarine arc caldera: Brothers volcano, Kermadec arc. Econ Geol 107:1557–1570. doi:10.2113/econgeo.107.8.1557

Embley RW, Resing J, Tebo B, Baker ET, Butterfield DA, Chadwick Jr WW, Davis R, de Ronde CEJ, Lilley MD, Lupton JE, Merle SG, Rubin KH, Shank TM, Walker SL, Arculus RJ, Bobbit AM, Buck N, Caratori Tontini F, Crowhurst PV, Mitchell E, Olson EJ, Ratmeyer V, Richards S, Roe K, Keener P, Maritnez-Lyons A, Sheehan C, Brian R (2013) Hyperactive hydrothermal activity in the NE Lau basin revealed by ROV dives. AGU. San Francisco

Giggenbach WF (1992) Isotopic shifts in waters from geothermal and volcanic systems along convergent plate boundaries and their origin. Earth Planet Sci Lett 113:495–510

Graham S, Pearson N, Jackson S, Griffin W, O'Reilly SY (2004) Tracing Cu and Fe from source to porphyry: in situ determination of Cu and Fe isotope ratios in sulfides from the Grasberg Cu-Au deposit. Chem Geol 207:147–169. doi:10.1016/j.chemgeo.2004.02.009

Gruen G, Weis P, Driesner T, de Ronde CEJ, Heinrich CA (2012) Fluid-flow patterns at Brothers volcano, southern Kermadec arc: insights from geologically constrained numerical simulations. Econ Geol 107:1595–1611. doi:10.2113/econgeo.107.8.1571

Gruen G, Weis P, Driesner T, Heinrich CA, de Ronde CEJ (2014) Hydrodynamic modeling of magmatic-hydrothermal activity at submarine arc volcanoes, with implications for ore formation. Earth Planet Sci Lett 404:307–318. doi:10.1016/j.epsl.2014.07.041

Haest M, Muchez P, Petit JCJ, Vanhaecke F (2009) Cu isotope ratio variations in the Dikulushi Cu-Ag deposit, DRC: of primary origin or induced by supergene reworking? Econ Geol 104:1055–1064. doi:10.2113/gsecongeo.104.7.1055

Haymon RM (1983) Growth history of hydrothermal black smoker chimneys. Nature 301:695–698. doi:10.1038/301695a0

Heinrich CA, Ryan CG, Mernagh TP, Eadington PJ (1992) Segregation of ore metals between magmatic brine and vapor: a fluid inclusion study using PIXE microanalysis. Econ Geol 87:1566–1583. doi:10.2113/gsecongeo.87.6.1566

Ikehata K, Hirata T (2012) Copper isotope characteristics of copper-rich minerals from the Horoman peridotite complex, Hokkaido, northern Japan. Econ Geol 107:1489–1497. doi:10.2113/econgeo.107.7.1489

Ikehata K, Notsu K, Hirata T (2011) Copper isotope characteristics of copper-rich minerals from besshi-type volcanogenic massive sulfide deposits, Japan, determined using a femtosecond LA-MC-ICP-MS. Econ Geol 106:307–316. doi:10.2113/econgeo.106.2.307

Jiang S, Jon W, Yu J, Pan J, Liao Q, Wu N (2002) A reconnaissance of Cu isotopic compositions of hydrothermal vein-type copper deposit, Jinman, Yunnan, China. Chin Sci Bull 47:247–250. doi:10.1360/02tb9059

Kim J, Son SK, Son JW, Kim KH, Shim WJ, Kim CH, Lee KY (2009) Venting sites along the Fonualei and Northeast Lau Spreading Centers and evidence of hydrothermal activity at an off-axis caldera in the northeastern Lau basin. Geochem J 43:1–13. doi:10.2343/geochemj.0.0164

Kim J, Lee KY, Kim JH (2011) Metal-bearing molten sulfur collected from a submarine volcano: implications for vapor transport of metals in seafloor hydrothermal systems. Geology 39:351–354. doi:10.1130/g31665.1

Kimball BE, Mathur R, Dohnalkova AC, Wall AJ, Runkel RL, Brantley SL (2009) Copper isotope fractionation in acid mine drainage. Geochim Cosmochim Acta 73:1247–1263. doi:10.1016/j.gca.2008.11.035

Larson PB, Maher K, Ramos FC, Chang Z, Gaspar M, Meinert LD (2003) Copper isotope ratios in magmatic and hydrothermal ore-forming environments. Chem Geol 201:337–350. doi:10.1016/j.chemgeo.2003.08.006

Li W, Jackson SE, Pearson NJ, Alard O, Chappell BW (2009) The Cu isotopic signature of granites from the Lachlan Fold Belt, SE Australia. Chem Geol 258:38–49. doi:10.1016/j.chemgeo.2008.06.047

Li W, Jackson SE, Pearson NJ, Graham S (2010) Copper isotopic zonation in the Northparkes porphyry Cu-Au deposit, SE Australia. Geochim Cosmochim Acta 74:4078–4096. doi:10.1016/j.gca.2010.04.003

Lowenstern JB, Mahood GA, Rivers ML, Sutton SR (1991) Evidence for extreme partitioning of copper into a magmatic vapor phase. Science 252:1405–1409

Lupton JE (1983) Terrestrial inert gases: isotope tracer studies and clues to primordial components in the mantle. Annu Rev Earth Planet Sci 11:371–414

Maher KC (2005) Analysis of copper isotope ratios by multi-collector inductively coupled plasma mass spectrometry and interpretation of copper isotope ratios from copper mineralization. Dissertation, Department of Geology. Washington State University, pp 249

Maher KC, Larson PB (2007) Variation in copper isotope ratios and controls on fractionation in hypogene skarn mineralization at Coroccohuayco and Tintaya, Peru. Econ Geol 102:225–237. doi:10.2113/gsecongeo.102.2.225

Maher KC, Jackson S, Mountain B (2011) Experimental evaluation of the fluid-mineral fractionation of Cu isotopes at 250 °C and 300 °C. Chem Geol 286:229–239. doi:10.1016/j.chemgeo.2011.05.008

Maréchal CN, Télouk P, Albarède F (1999) Precise analysis of copper and zinc isotopic compositions by plasma-source mass spectrometry. Chem Geol 156:251–273. doi:10.1016/S0009-2541(98)00191-0

Markl G, Lahaye Y, Schwinn G (2006) Copper isotopes as monitors of redox processes in hydrothermal mineralization. Geochim Cosmochim Acta 70:4215–4228. doi:10.1016/j.gca.2006.06.1369

Marty B, Dauphas N (2003) The nitrogen record for crust-mantle interaction and mantle convection from Archean to present. Earth Planet Sci Lett 206:397–410. doi:10.1016/s0012-821x(02)01108-1

Mason TFD, Weiss DJ, Chapman JB, Wilkinson JJ, Tessalina SG, Spiro B, Horstwood MSA, Spratt J, Coles BJ (2005) Zn and Cu isotopic variability in the Alexandrinka volcanic-hosted massive sulphide (VHMS) ore deposit, Urals, Russia. Chem Geol 221:170–187. doi:10.1016/j.chemgeo.2005.04.011

Massoth GJ, de Ronde CEJ, Lupton JE, Feely RA, Baker ET, Lebon GT, Maenner SM (2003) Chemically rich and diverse submarine hydrothermal plumes of the southern Kermadec volcanic arc (New Zealand). In: Larter RD, Leat PT (eds) Intra-oceanic subduction systems: tectonic and magmatic processes. Geological Society of London, London, pp 119–139

Mathur R, Ruiz J, Titley S, Liermann L, Buss H, Brantley S (2005) Cu isotopic fractionation in the supergene environment with and without bacteria. Geochim Cosmochim Acta 69:5233–5246. doi:10.1016/j.gca.2005.06.022

Mathur R, Titley S, Barra F, Brantley S, Wilson M, Phillips A, Munizaga F, Maksaev V, Vervoort J, Hart G (2009a) Exploration potential of Cu isotope fractionation in porphyry copper deposits. J Geochem Explor 102:1–6. doi:10.1016/j.gexplo.2008.09.004

Mathur R, Titley S, Hart G, Wilson M, Davignon M, Zlatos C (2009b) The history of the United States cent revealed through copper isotope fractionation. J Archaeol Sci 36:430–433. doi:10.1016/j.jas.2008.09.029

Mathur R, Ruiz J, Casselman MJ, Megaw P, van Egmond R (2012) Use of Cu isotopes to distinguish primary and secondary Cu mineralization in the Cañariaco Norte porphyry copper deposit, northern Peru. Miner Deposita 47:755–762. doi:10.1007/s00126-012-0439-y

Mathur R, Munk L, Nguyen M, Gregory M, Annell H, Lang J (2013) Modern and paleofluid pathways revealed by Cu isotope compositions in surface waters and ores of the Pebble porphyry Cu-Au-Mo deposit, Alaska. Econ Geol 108:529–541. doi:10.2113/econgeo.108.3.529

Mavrogenes JA, Berry AJ, Newville M, Sutton SR (2002) Copper speciation in vapor-phase fluid inclusions from the Mole Granite, Australia. Am Mineral 87:1360–1364

Migdisov AA, Bychkov A, Williams-Jones AE, van Hinsberg VJ (2014) A predictive model for the transport of copper by HCl-bearing water vapor in ore-forming magmatic-hydrothermal systems: implications for copper porphyry ore formation. Geochim Cosmochim Acta 129: 33–53. doi:10.1016/j.gca.2013.12.024

Mirnejad H, Mathur R, Einali M, Dendas M, Alirezaei S (2010) A comparative copper isotope study of porphyry copper deposits in Iran. Geochem-Explor Env A 10:413–418. doi:10.1144/1467-7873/09-229

Palacios C, Rouxel O, Reich M, Cameron EM, Leybourne MI (2011) Pleistocene recycling of copper at a porphyry system, Atacama Desert, Chile: Cu isotope evidence. Miner Deposita 46:1–7. doi: 10.1007/s00126-010-0315-6

Paton C, Hellstrom J, Paul B, Woodhead J, Hergt J (2011) Iolite: freeware for the visualisation and processing of mass spectrometric data. J Anal At Spectrom 26:2508–2518. doi:10.1039/c1ja10172b

Rempel KU, Liebscher A, Meixner A, Romer RL, Heinrich W (2012) An experimental study of the elemental and isotopic fractionation of copper between aqueous vapor and liquid to 450 °C and 400 bar in the CuCl-NaCl-H_2O and CuCl-NaHS-NaCl-H_2O systems. Geochim Cosmochim Acta 94:199–216. doi:10.1016/j.gca.2012.06.028

Rouxel O, Fouquet Y, Ludden JN (2004) Copper isotope systematics of the Lucky Strike, Rainbow, and Logatchev sea-floor hydrothermal fields on the Mid-Atlantic Ridge. Econ Geol 99:585–600. doi:10.2113/99.3.585

Seo JH, Lee SK, Lee I (2007) Quantum chemical calculations of equilibrium copper (I) isotope fractionations in ore-forming fluids. Chem Geol 243:225–237. doi:10.1016/j.chemgeo.2007.05.025

Sherman DM (2013) Equilibrium isotopic fractionation of copper during oxidation/reduction, aqueous complexation and ore-forming processes: predictions from hybrid density functional theory. Geochim Cosmochim Acta 118:85–97. doi:10.1016/j.gca.2013.04.030

Von Damm KL (1995) Controls on the chemistry and temporal variability of seafloor hydrothermal fluids In: Humphris SE, Sierenberg RA, Mullineaux LS, Thompson RE (eds) Seafloor hydrothermal systems: physical, chemical, biological, and geological interactions. American Geophysical Union, pp 222–247

Zhu XK, O'Nions RK, Guo Y, Belshaw NS, Rickard D (2000) Determination of natural Cu-isotope variation by plasma-source mass spectrometry: implications for use as geochemical tracers. Chem Geol 163:139–149. doi:10.1016/S0009-2541(99)00076-5